



## NRC Publications Archive Archives des publications du CNRC

### **Settlement observations at Kars Bridge** Eden, W. J.; Poorooshasb, H. B.

This publication could be one of several versions: author's original, accepted manuscript or the publisher's version. /  
La version de cette publication peut être l'une des suivantes : la version prépublication de l'auteur, la version  
acceptée du manuscrit ou la version de l'éditeur.

#### **Publisher's version / Version de l'éditeur:**

*Canadian Geotechnical Journal*, 5, 1, pp. 28-45, 1968-04-01

#### **NRC Publications Record / Notice d'Archives des publications de CNRC:**

<https://nrc-publications.canada.ca/eng/view/object/?id=e5aa2004-7d97-40f6-a012-45287eadc011>  
<https://publications-cnrc.canada.ca/fra/voir/objet/?id=e5aa2004-7d97-40f6-a012-45287eadc011>

Access and use of this website and the material on it are subject to the Terms and Conditions set forth at  
<https://nrc-publications.canada.ca/eng/copyright>  
READ THESE TERMS AND CONDITIONS CAREFULLY BEFORE USING THIS WEBSITE.

L'accès à ce site Web et l'utilisation de son contenu sont assujettis aux conditions présentées dans le site  
<https://publications-cnrc.canada.ca/fra/droits>  
LISEZ CES CONDITIONS ATTENTIVEMENT AVANT D'UTILISER CE SITE WEB.

**Questions?** Contact the NRC Publications Archive team at  
PublicationsArchive-ArchivesPublications@nrc-cnrc.gc.ca. If you wish to email the authors directly, please see the  
first page of the publication for their contact information.

**Vous avez des questions?** Nous pouvons vous aider. Pour communiquer directement avec un auteur, consultez la  
première page de la revue dans laquelle son article a été publié afin de trouver ses coordonnées. Si vous n'arrivez  
pas à les repérer, communiquez avec nous à PublicationsArchive-ArchivesPublications@nrc-cnrc.gc.ca.



Ser  
TH1  
N21r2  
no. 362  
c. 2  
  
BLDG

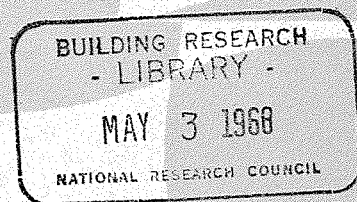
17218  
ANALYZED

NATIONAL RESEARCH COUNCIL OF CANADA  
CONSEIL NATIONAL DE RECHERCHES DU CANADA

SETTLEMENT OBSERVATIONS AT KARS BRIDGE

W. J. EDEN and H. B. POOROOSHASB

Reprinted from  
CANADIAN GEOTECHNICAL JOURNAL  
Vol. V, No. 1, February 1968  
pp. 29-46



Research Paper No. 362  
of the  
Division of Building Research

OTTAWA  
April 1968

Price 25 cents

NRC 10086

## ANALYZED

### SETTLEMENT OBSERVATIONS AT KARS BRIDGE

W. J. EDEN *Division of Building Research, National Research Council of Canada*

H. B. POOROOSHASB *Visiting Scientist, Soil Mechanics Section, Division of Building Research, National Research Council of Canada*

A 26 ft. high approach fill was constructed in November 1959 for a bridge over the Rideau river near Kars, Ontario. The fill was placed over 50 ft. of Leda clay, the lower 30 ft. of which was extremely sensitive and compressible. Prior testing indicated that the preconsolidation pressure of the clay would be exceeded.

Settlement gauges and piezometers under the fill have been observed since the start of construction. After 7½ years, 20 in. of settlement has occurred under the centre of the fill. Settlements are continuing at an appreciable rate although the excess pore water pressure has dissipated to a low level and is nearly constant through the clay layer.

The field observations of settlement and pore water pressure are compared with values calculated and a closed form solution to the process of consolidation obtained by a heat balance integral technique and by considering the clay layer to be a rigid plastic.

Un remblai d'approche de 26 pieds de hauteur fut construit en novembre 1959 pour un pont sur la rivière Rideau près de Kars en Ontario. Ce remblai fut érigé sur une couche d'argile Leda profonde de 50 pieds dont les 30 pieds de base étaient extrêmement sensibles et compressibles. Des essais avaient démontré que les pressions de préconsolidation seraient dépassées.

Depuis le début des travaux et jusqu'à ce jour des lectures ont été faites tant sur des jauges de tassement que sur des piézomètres placés sous le remblai. Ces lectures révèlent qu'il s'est produit au cours des 7½ dernières années, 20 pouces de tassement au centre du remblai et que ces tassements s'effectuent toujours à un rythme appréciable en dépit du fait que les pressions interstitielles aient présentement atteint un niveau moindre et soient de presque égale intensité à travers la couche d'argile.

On compare les observations in situ des tassements et de la pression interstitielle avec les valeurs calculées en utilisant une solution explicite du problème de consolidation obtenue par la technique de l'intégrale de l'équilibre calorifique et en considérant que la couche d'argile se comporte comme un matériau rigide plastique.

The Kars bridge is situated about 25 miles south of Ottawa. The bridge was erected over the Rideau river in 1961 by Carleton county, to replace a low-level swing bridge. To meet the Department of Transport's clearance requirements over the Rideau canal, a fixed span required a 26 ft. approach fill on the west side of the river where low-lying swampland is underlain by soft Leda

clay. The 26 ft. fill was heavy enough to cause concern about the stability of the proposed embankment and could be expected to cause settlements of the order of 2 ft. With the co-operation of the County Engineer for Carleton, the Division of Building Research of the National Research Council of Canada undertook a testing and instrumentation program on the fill. The results of this program are presented herein.

#### THE SITE

On the west side, the soil profile consists of a 3 ft. surface layer of peat, 5 ft. of sandy clay alluvium, 12 ft. of over-consolidated fissured clay, 30 ft. of extremely sensitive soft Leda clay and, finally, 3 to 5 ft. of glacial till over the shale bedrock. Figure 1 is a log on which are plotted results of the soil tests from one boring. Because of stability considerations, the fill was built in two stages. The first lift of 20 ft. was placed in November 1959. The pile-founded west abutment was constructed during the following spring and the final 6 ft. of fill were placed in June 1961. The anticipated increase in vertical stress due first to the 20 ft. fill and later to the 26 ft. fill is indicated on Figure 1 by lines C-C and D-D respectively. It was estimated that the 20 ft. fill would exceed the preconsolidation pressure and cause appreciable consolidation in the clay layer.

#### *Instrumentation*

In a previous paper (Eden 1960), a detailed description of the instrumentation at the Kars bridge was given. Figure 2 is a plan and side elevation of the area showing the location of the instrumentation. It includes a row of settlement gauges along the centreline of the fill at depths of 20, 25, 30, 35, and 40 ft. with a deep bench mark founded on bedrock at 55 ft. The depths were chosen in order to divide the compressible clay zone into increments of about 5 ft. To measure settlements across the fill, five 3 ft.  $\times$  4 ft.  $\times$   $\frac{1}{8}$  in. steel plates were placed on the first lift of the fill and carefully levelled. These were later located by drilling through the fill; then vertical cased rods were set on them. The steel plates were located on the centreline, 12½ ft. south of centreline, 25 ft. south of centreline (shoulder of fill), 49 ft. south of centreline (mid slope), and 74 ft. south (at the toe).

Fifteen Geonor piezometers were installed to monitor changes in pore water pressure during and after loading. Seven of the piezometers were located on centreline at depths of 9, 16, 23, 28, 33, 38, and 48 ft. below original grade. Three piezometers at depths of 15, 20, and 35 ft. were located on the shoulder line of the first stage of fill. Three more, at depths of 15, 20, and 30 ft., were located at the toe of the fill, and two piezometers at depths of 20 and 25 ft. were located beyond the toe, 100 ft. south of centreline. To ensure that a minimum of volume change would influence the piezometer readings, those on centreline were terminated in a manhole formed of a 5 ft. diameter corrugated steel culvert section rising 11 ft. above original grade. These piezometers were connected to Bourdon gauges during the loading phase and for two months after the load application when they remained under a positive head. Water

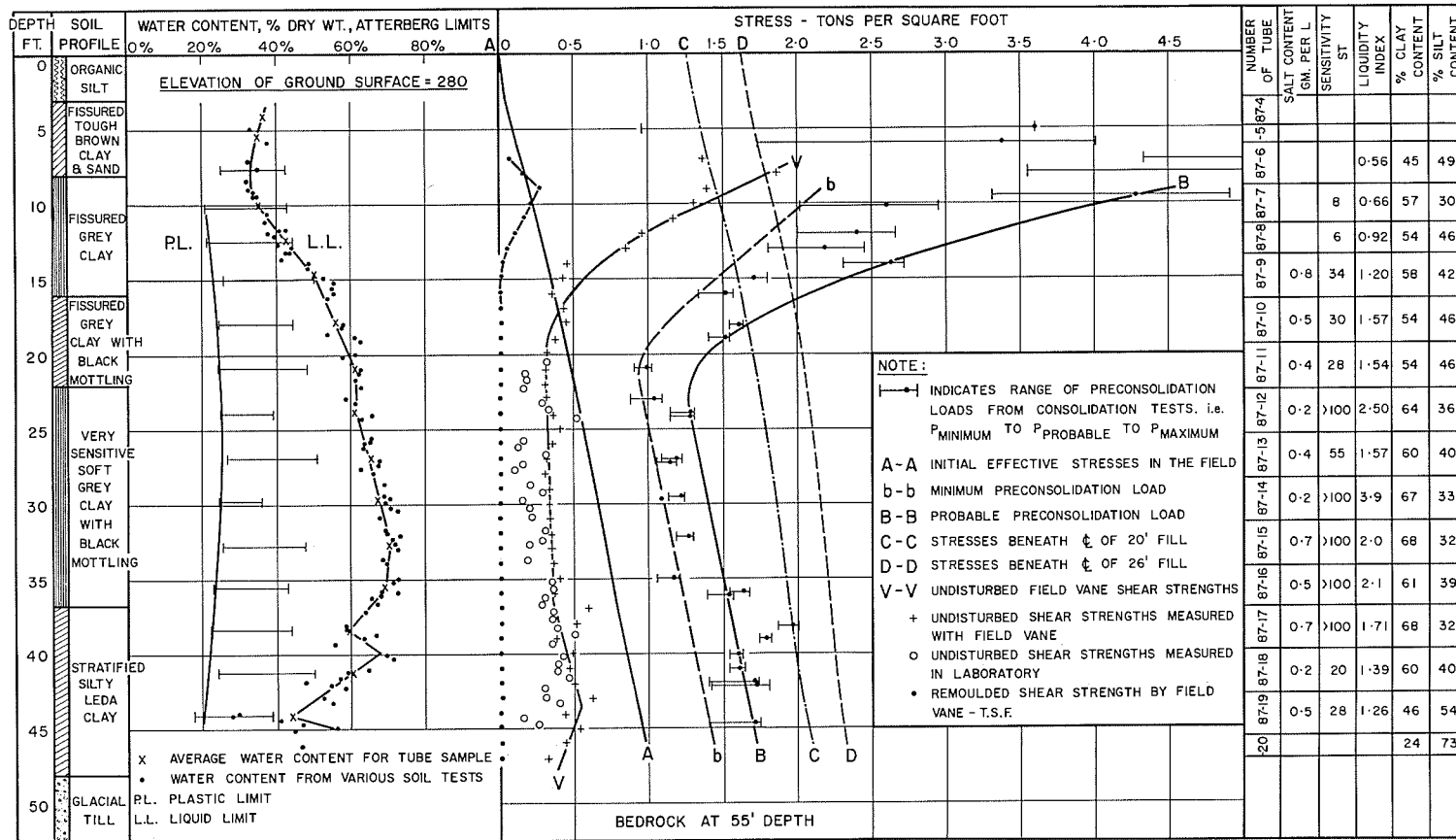


FIGURE 1. Boring log showing test results and stress distributions under the approach fill at Kars

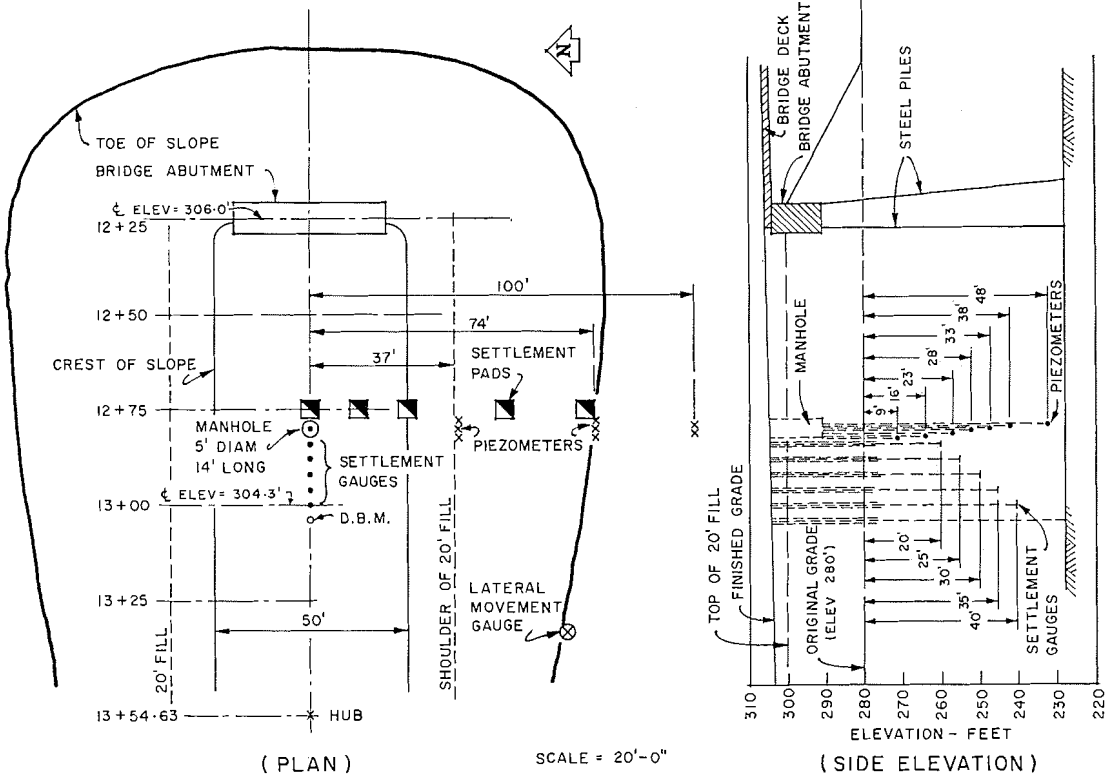


FIGURE 2. Layout of instrumentation for Kars bridge fill

levels were determined with an electrical probe in the open small volume stand pipes.

To check the response of piezometers, three piezometers at 30 and 35 ft. were checked in June 1963. The piezometers were filled with water to the top of the tube, and the time required for the piezometers to revert to their original level was recorded. In each case, after three days the piezometric level had returned to within 10 per cent of its former level. In a week, the former level had been reached.

At the toe of the fill, a 2½ in. diameter flexible plastic pipe was installed vertically through the clay layer. The purpose of this pipe was to detect lateral movements. Readings were taken by lowering a lighted plumb bob down the tube. The position of the plumb bob at predetermined depths was measured from the top of the pipe which was, in turn, measured from a fixed point 100 ft. from the fill. With this system, it was believed that movements of more than ⅛ in. could be detected.

OBSERVATIONS

*Settlements*

Construction on the site began on 1 November 1959. The first step was to remove the organic silt with a dragline and fill up to grade level with a sand

fill. The excavation and backfill were completed by 7 November 1959, at which stage very little load had been added. From 9 to 24 November, the first 20 ft. of the fill were built up by the contractor on a  $5\frac{1}{2}$  day per week schedule. While the filling operation proceeded, extensions were added to the centreline settlement gauges. It was estimated that a  $\frac{1}{8}$  in. error could occur at each joint. The settlement records indicate in Figure 3 that little immediate settlement occurred

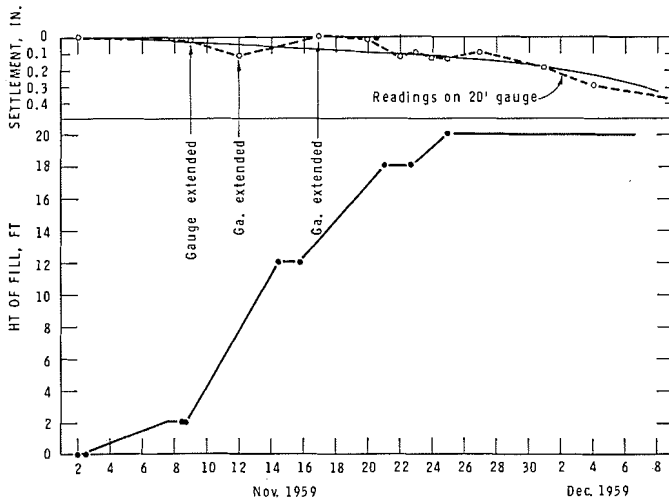


FIGURE 3. Rate of load application (first stage) and initial settlements

during the loading operations. Since three extensions were necessary for the settlement gauge, the maximum possible immediate settlement was about 0.3 in. Figure 4 shows the settlement records over a  $7\frac{1}{2}$  year period. By April 1967 a total settlement of 19.7 in. was recorded under the centreline. Figure 5 indicates the transverse distribution of the settlement.

#### *Pore water pressures*

When loading began, the piezometers showed an immediate response to the change in stresses. Those along the centreline were equipped with bourdon gauges on 16 November. Maximum pore water pressure was measured on the centreline piezometer located 28 ft. below grade on 23 November, the final day of load application. Pressure then dropped off rapidly to a relatively constant value and has dissipated slowly since then. Figure 6 shows equipotential contours of the maximum excess pore water pressure measured on 23 November 1959. The contours for 2 February 1960 are also shown (in dashed lines), at which time the excess pore water pressure levelled off. Figure 7 shows the variation of pore water pressures with time for three of the centreline piezometers. The rising of the Rideau river to flood stage in April 1960 was reflected. In June 1960, the driving of the piles for the west abutment about 50 ft. away caused a temporary rise in piezometric levels. Finally, in June 1961 fill was added, bringing the road to final grade. Since June 1961 the

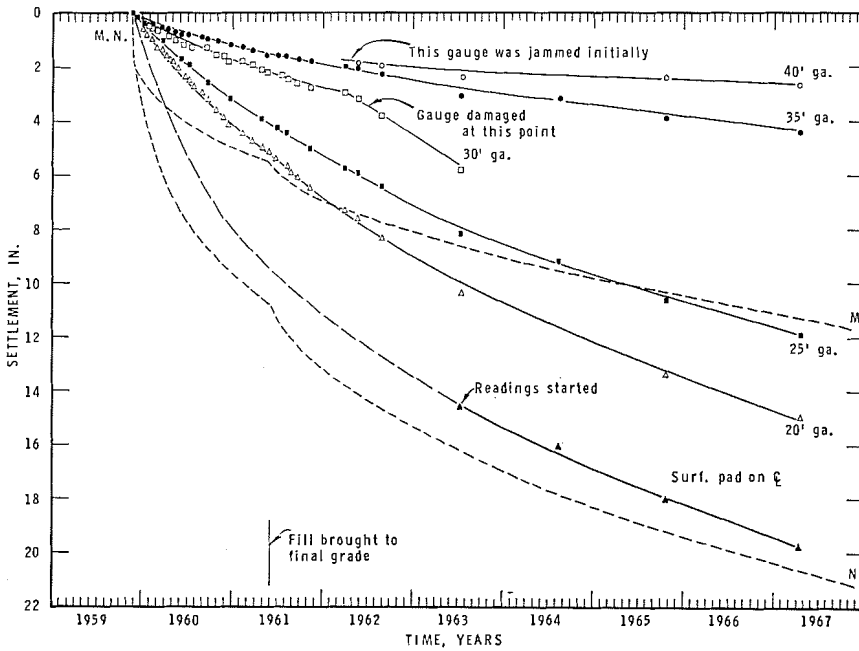


FIGURE 4. Observed settlements

loading has been constant and the pore water pressures have slowly dissipated to an excess head of about 5 ft.

*Lateral movements*

Surveys in the 2½ in. plastic pipe were continued from November 1959 until July 1963. During this time, it was possible to observe the plumb bob to depths of 45 ft., indicating that lateral movements were small. Because of

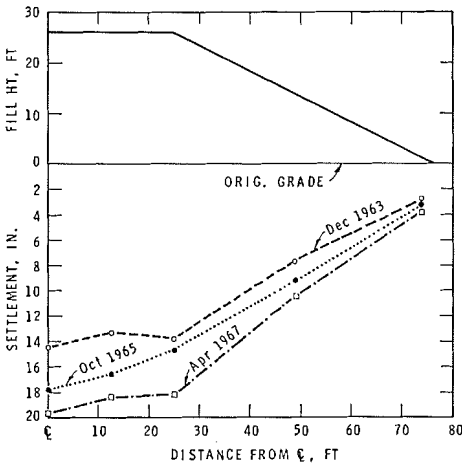


FIGURE 5. Observations of transverse settlements



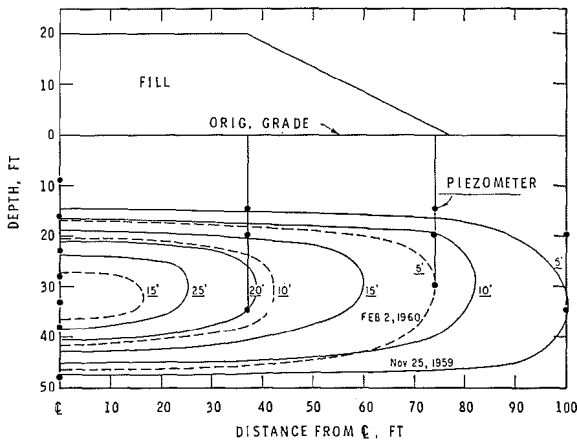


FIGURE 6. Equipotential contours of excess pore water pressure at end of loading and two months later

difficulties in maintaining a stable reference pin, the absolute accuracy of the measurements is somewhat doubtful. The total movement, in any case, does not appear to have exceeded one-half inch. It may be concluded that lateral movements were relatively insignificant compared with the vertical movements.

#### TESTING AND SETTLEMENT PREDICTIONS

Several field vane borings were made on the site. The results of these tests are shown on Figure 1. Continuous samples were taken with an NGI piston sampler from two other borings. On these samples a comprehensive program of consolidation testing was undertaken, the object being to determine the preconsolidation pressure of the clay and to obtain coefficients of consolidation in order to predict settlement.

Two types of consolidation test were employed. Sixty-seven standard incremental loading consolidation tests were conducted on samples from the two borings. The results of the preconsolidation determinations are shown on Figure 1. The minimum and probable assumed preconsolidation pressures for the most compressible layer, from 23 to 37 ft., are shown by lines *b-b* and *B-B*. For settlement calculations, the probable values (*B-B*) were used.

A second series of consolidation tests was conducted for settlement calculations by the method suggested by Skempton and Bjerrum (1957). In these tests the specimen was first loaded to the initial effective overburden pressure. The next loading increment increased the effective pressure to the calculated effective pressure under the 20 ft. fill and the final increment to the pressure under the 26 ft. fill. These tests yielded coefficients of compressibility and consolidation over the working load range.

For purposes of the settlement predictions, it was assumed that the fissured crust extended to a depth of 23 ft. and that settlements in the crust would be generally confined to a layer between 18 and 23 ft., where the weight of the

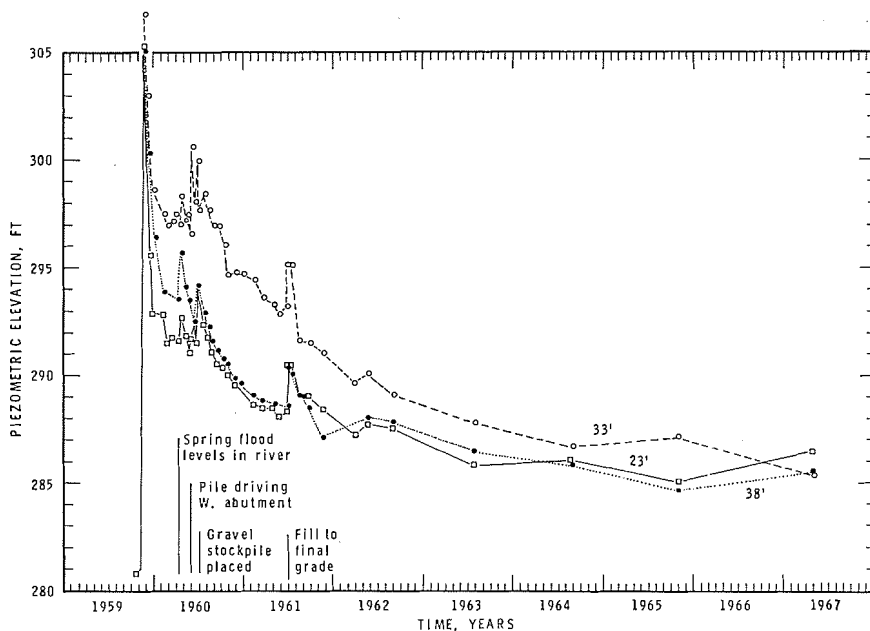


FIGURE 7. Changes in levels of three piezometers with time (datum 280.0 ft.)

fill exceeded the preconsolidation load. It was further assumed there was a drainage sink at 18 ft. in the fissured crust of the clay. The second layer, from 23 to 37 ft., is rather uniform, highly sensitive, and quite compressible clay. In the third layer, from 37 to 46 ft., the clay is more stratified and somewhat less compressible. Since the permeability of the lower layer, determined from consolidation tests, is more than twice that of the middle layer, the bottom drainage sink for the middle layer was assumed to be at 37 ft. The lower layer was assumed to drain towards the bottom, at a depth of 46 ft. Two estimates of settlement were made, based on the two types of test. Method A, using the standard type of test, gave four phases of settlement:

- (1) immediate or elastic settlement based on modulus of compression determined from undrained triaxial tests;
- (2) recompression settlements caused by increase of stress from the existing effective overburden pressure to the preconsolidation pressure;
- (3) settlements due to the normal consolidation process along the virgin branch of the pressure void ratio curve from preconsolidation pressure to pressure due to load of a 20 ft. fill; and
- (4) settlements due to increase of load from 20 to 26 ft. fill.

The rate of settlement determined by this method is shown on Figure 4 as line *M-M*. The method suggested by Skempton and Bjerrum is shown on Figure 4 as line *N-N*. This method yielded about the same total amount of settlement (35 in.) as the first method (37 in.), but the time required for 100 per cent consolidation was much less—27 years as compared with 80 years.

The rate of settlement depends upon values of  $c_v$  and  $a_v$  measured in laboratory tests known to have a limited accuracy. The influence of the fissured crust

in distributing the load laterally and the location of drainage sinks in the field are additional uncertain factors.

For the middle clay zone the pressure-void ratio curves have the characteristic shape of extremely sensitive clays. Figure 8 illustrates a typical curve for test No. 87-28-12 from a depth of 26 ft. This specimen was loaded in small increments, a procedure recommended by Hamilton and Crawford (1959). Figure 9 shows the time-compression curves for the various load increments during the test. It will be seen that in the region of the preconsolidation pressure, the time-compression curves do not have a well-defined primary and secondary stage but that the rate of compression appears to be mainly influenced by a structural breakdown mechanism. As the void ratio decreases, the structural breakdown process is no longer as significant, and better defined primary and secondary stages can be recognized. Using conventional procedures for interpreting the time-compression curves, Table I lists the coefficients of compressibility ( $a_v$ ), consolidation ( $c_v$ ), and permeability ( $k$ ) determined from the test.

The coefficients vary widely and do not follow any logical pattern with decreasing void ratio and, for a purely hydrodynamic process of consolidation, may be misleading (Raymond 1966). Crawford (1964) has indicated that "structural breakdown" is an important feature in the compression of Leda

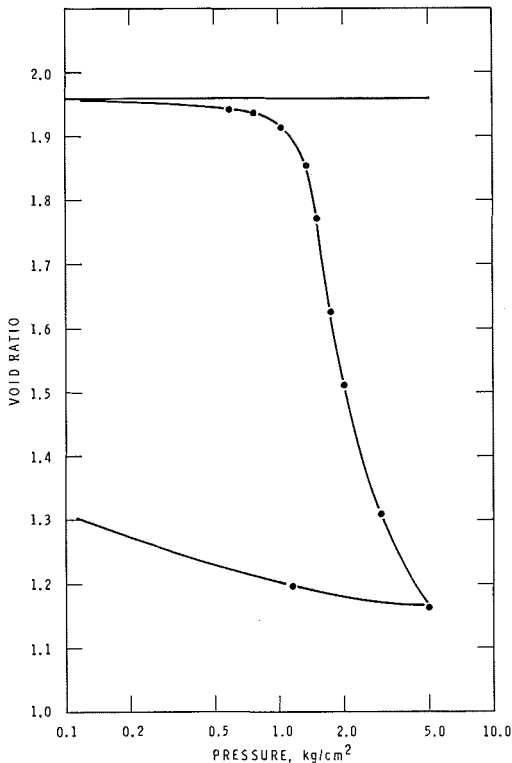


FIGURE 8. Pressure-void ratio curves, sample 87-28-12, depth 26 ft. 0 in.

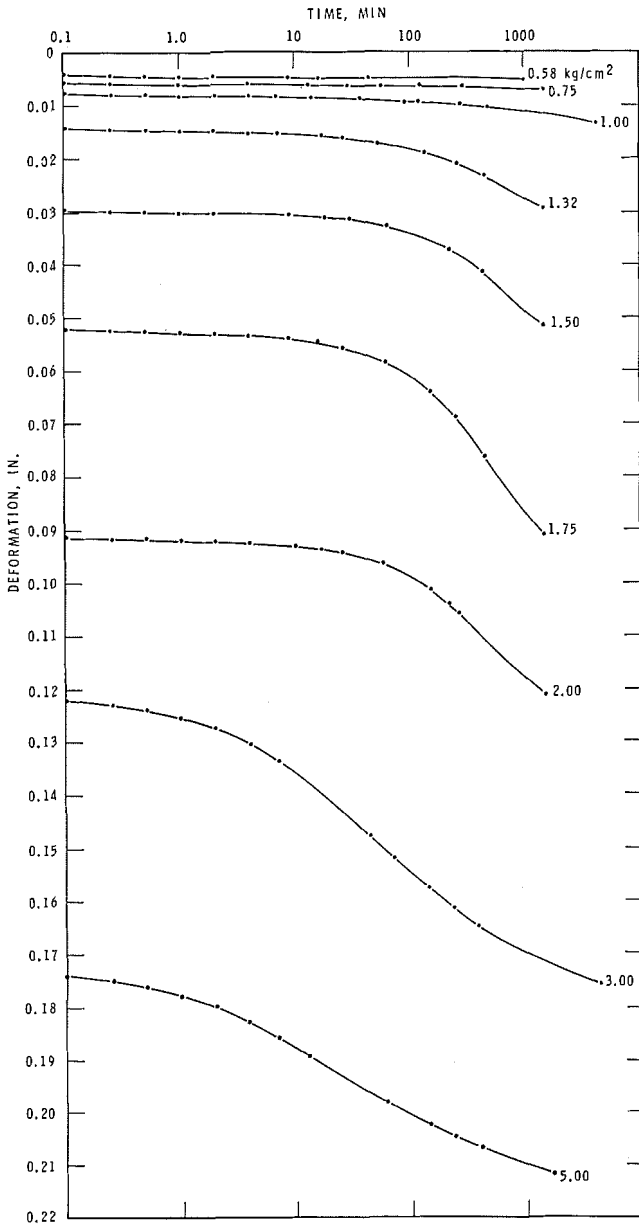


FIGURE 9. Time deformation curves, sample 87-28-12

clay, particularly near the preconsolidation pressure. If the laboratory test is regarded as a model of field behaviour, then the coefficients of compression and consolidation should be determined from the working stress range. Because of the shape of the time-compression curves in this region, with compression continuing over a long period of time little confidence can be placed in the laboratory values of coefficients, and agreement between the field rate and the

TABLE I

Coefficients derived from test No. 87-28-12

| Pressure<br>kg/cm <sup>2</sup> | $a_v$ cm <sup>2</sup> /kg | $c_v$ cm <sup>2</sup> /min. $\times 10^{-3}$ | $K$ cm/sec. $\times 10^{-6}$ |
|--------------------------------|---------------------------|--|------------------------------|
| 0.75                           | .0412                     | .48  | .0813                        |
| 1.00                           | .0902                     | .49  | .0257                        |
| 1.32                           | .1844                     | .79  | .0850                        |
| 1.50                           | .4611                     | .60  | .1664                        |
| 1.75                           | .5880                     | .67  | .2502                        |
| 2.00                           | .4520                     | .92  | .2760                        |
| 3.00                           | .2020                     | .51  | .8033                        |
| 5.00                           | .0725                     | .25  | .8515                        |

predicted rate, if achieved, may be fortuitous. The fact that method B seems to give better agreement may be because the load increments used duplicate the field situation more closely than the conventional test. With this type of test, the problem of interpretation of the laboratory time-compression curve remains. The average values determined will depend on the number of tests, and the manner in which the individual time-compression curves are interpreted.

The presence of the fissured crust of clay tends to distribute the load laterally. The compressibility of the fissured crust is unknown, but for purposes of the calculations it was assumed to be relatively incompressible and settlement gauges were not installed within the crust. The difference in settlement between the surface pad and the 20 ft. gauge is a measure of the compression in this zone, and it is seen to be more compressible than originally assumed. It was also assumed that the fissured crust would provide an upper drainage sink but the field pore water pressure measurements indicate that the drainage sink was somewhere above 16 ft.

All piezometers in the compressible clay zone behaved in a similar manner—a rapid response to the loading followed by a rapid dissipation to about 15 ft. excess head, followed by a relatively slow rate of dissipation. Eventually, no significant difference in head was evident between the piezometers in the middle of the clay (28 and 33 ft.) and those near the boundaries of the layer (23 and 38 ft.).

In considering the actual behaviour of the fill, an attempt was made to treat the case by assuming that the clay layer could be considered as a rigid plastic material and that a closed form solution to the process of consolidation could be obtained by using a heat balance integral technique. The basis for this treatment is outlined in Appendix A.

By assuming the clay to be a rigid plastic material, the ratio of the coefficients of consolidation up to and beyond the preconsolidation pressure ( $\alpha_1$  and  $\alpha_2$ ) becomes zero. To calculate the dissipation of pore water pressure due to Phase III of the process (see Appendix), a value of  $\alpha_2$  was required from the laboratory tests. As the working stress range in the field involved the region of "structural breakdown" in the laboratory tests, the value to be used had to be decided upon. It was reasoned that the structural breakdown would also occur in

the field and that the  $c_v$  values from laboratory tests should therefore be determined from the working stress range. The results of 57 tests from two borings were assembled (Figure 10) and a value of  $c_v$  or  $\alpha_2 = .001 \text{ cm}^2/\text{min}$ . was chosen. Calculations were made for the dissipation of pore water pressure at a depth of 23 ft. These calculations are presented in Figure 11, and may be compared with those of the 23 ft. piezometer, also shown in Figure 11.

In comparing the observed and calculated pressures, the following features should be noted. The load addition caused a rapid rise in pore water pressure, which quickly dissipated to a value  $v$ . This was followed by the consolidation (Phase III) process in which the pore water pressures dissipated slowly with time. The fact that the rate of dissipation shown in Figure 11 agrees with the observed measurements suggests that the value selection for  $c_v$  of  $0.001 \text{ cm}^2/\text{min}$ . was reasonable.

If the drainage of the clay layer proceeded as assumed in a vertical direction, then piezometers at 28 and 33 ft. should have shown a significant gradient towards the 23 and 38 ft. levels. Since this is not the case, either lateral drainage must have been great or significant pore pressures are created by structural breakdown of the soil. A study of careful photographic records of continuous samples of the soil profile revealed no permeable layers. There might have been small imperfections in the clay, such as minor sand or silt parting, or fissures, which escaped detection. If one examines the piezometric gradients (Figure 6) there does not seem to be a significant tendency for lateral drainage. Thus, the rate of consolidation in the region of structural breakdown of Leda clay may not be entirely dependent on the field permeability, but rather on the viscous type of structural breakdown. Jarret (1967) has demonstrated this phenomenon in laboratory test specimens, and has suggested that the consolidation of Leda clay has three phases: (1) an elastic deformation range up to the preconsolidation pressure; (2) a structural collapse governed by a form of structural viscosity at and beyond the preconsolidation pressure; and (3) a normal process of primary consolidation with a definite relation between pressure and void ratio. It is suggested that the second phase accounts for a significant part of the settlements at the Kars site, and that this accounts for

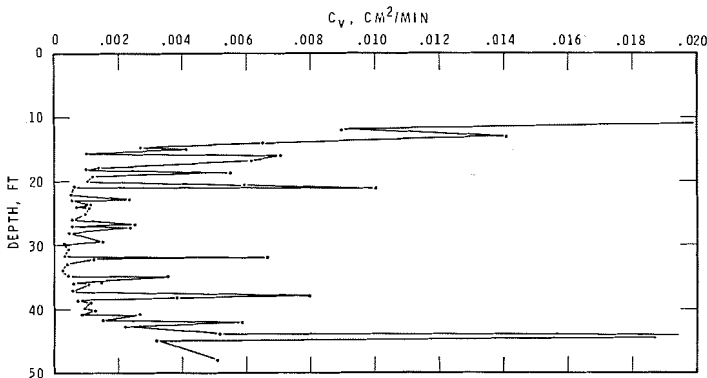


FIGURE 10. Variation in  $c_v$  with depth;  $c_v$  determined at loads just beyond  $P_N$

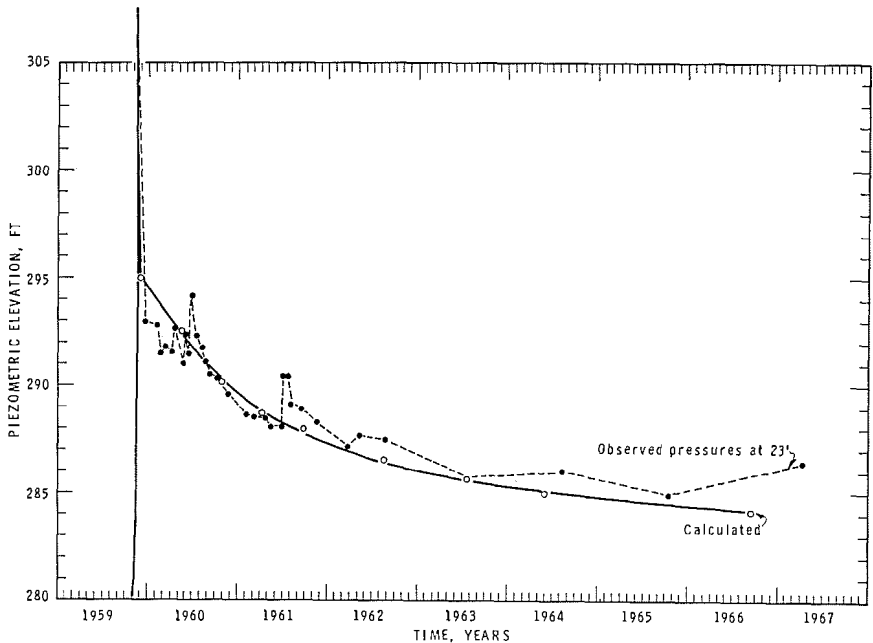


FIGURE 11. Calculated pore water pressure dissipation for 23 ft. level

the uniform pore water pressures being measured in the clay layer at the present time.

#### CONCLUSIONS

The observations at the Kars bridge approach fill demonstrate the field behaviour of a layer of highly compressible, lightly overconsolidated Leda clay under a relatively wide load which exceeded the preconsolidation pressure. The observations suggest that:

- (1) Because the amount of settlement measured in the field is not greater than predicted, a liberal interpretation can be placed on the value of preconsolidation pressure determined in the laboratory on tube samples taken by refined sampling techniques.
- (2) Immediate or elastic settlements in this clay are very slight and the clay had a high modulus of deformation so that it could be considered a "rigid plastic material."
- (3) No significant lateral strain or spreading was observed.
- (4) The fissured crust of the Leda clay appears to be more compressible and not as free draining as had been originally assumed.
- (5) Predictions of settlement on the basis of laboratory tests are difficult due to the structural breakdown of the clay structure in the region of the preconsolidation pressure. By using values of the coefficient of consolidation determined somewhat arbitrarily from laboratory tests from the working stress range, reasonable agreement has been achieved between the field rate of consolidation and the theoretical treatment.

## ACKNOWLEDGMENTS

The Kars bridge project required the assistance of most of the staff of the Soil Mechanics Section in the preparation and installation of the field instruments and in the extensive laboratory testing program. Particular acknowledgment is due to M. Bozozuk who conducted the initial analysis of settlement. The project was given the full and continued cooperation of the County Engineer of Carleton County, initially Mr. A. J. Graham, and subsequently Mr. G. Weatherall. This paper is a contribution of the Division of Building Research of the National Research Council and is published with the approval of the Director.

## REFERENCES

- CRAWFORD, C. B., 1964. Interpretation of the consolidation test. *JSM&FD, Proc. ASCE 90*, SM 5: 87-102.
- EDEN, W. J., 1961. Field studies of the consolidation properties of Leda clay. *Proc. 14th Can. Soil Mechanics Conf.*, Assoc. Committee Soil and Snow Mechanics, NRC TM 69.
- HAMILTON, J. J., and CRAWFORD, C. B., 1959. Improved determination of preconsolidation pressure on a sensitive clay. *ASTM STP 254*: 254-70.
- JARRETT, P. M., 1967. Time-dependent consolidation of a sensitive clay. *ASTM Materials Research and Standards 7*, 7: 300-4.
- RAYMOND, G. P. 1966. Consolidation of slightly overconsolidated soils. *JSM&FD, Proc. ASCE 92*, SM 5: 1-20.
- SKEMPTON, A. W., and BJERRUM, L., 1957. A contribution to the settlement analysis of foundations on clay. *Géotechnique 7*, 4: 168-78.

## APPENDIX A: SOLUTION TO A NON-LINEAR CONSOLIDATION PROBLEM

This note discusses the nature of consolidation of a slightly overconsolidated clay layer when subjected to a pressure higher than its preconsolidation value. The method used for the analysis employs an expression analogous to the "heat balance integral" used in heat transfer problems. As an extensive account of the method is already given by Goodman (1964), only a brief account will be presented here. It is convenient to start by giving a concise statement of the problems to be discussed.

A clay layer of thickness  $h$ , underlain by bedrock and free-draining on its upper surface, is subjected to a load of  $\sigma_f I(t)$  where  $\sigma_f$  is constant and  $I(t)$  is the unit step function. For times  $t < 0$  the effective stress in the layer is  $\sigma_i$ , also a constant, and its excess pore water pressure  $u$  is assumed to be equal to zero. The clay is initially overconsolidated and the loading is such that,

$$(1) \quad \sigma_i < \sigma_0 < \sigma_f$$

where  $\sigma_0$  denotes the preconsolidation pressure of the layer. The distribution and variation of the pore water pressure as a function of time and position must be obtained.

The origin of the co-ordinate system is taken at the top surface of the layer and the  $z$  axis is taken vertically pointing downwards.

Shortly after the application of the load, the uppermost portion of the layer (i.e., in the vicinity of  $z \approx 0$ ) would have consolidated fully so that



$$(2) \quad u = -\sigma' + \sigma_i + \sigma_f = 0$$

where  $\sigma'$  represents the effective stress. At this level and up to a level  $z = s(t)$  where

$$(3) \quad \sigma' = \sigma_i + \sigma_f - \mu = \sigma_0,$$

the material becomes normally consolidated (since in this zone  $\sigma' \geq \sigma_0$ ) whereas for  $h \geq z > s(t)$ , the clay is still overconsolidated. In other words,  $s(t)$  signifies the elevation at which the material changes its nature from overconsolidated to normally consolidated. Another elevation which is also of importance in the subsequent analysis is  $s$ , the level of influence  $i(t)$ . This is defined as the depth below which the clay has not as yet felt the effect of surface loading. (The corresponding terminology in heat transfer is the penetration distance.) Obviously, both  $s$  and  $i$  are non-decreasing functions of time that assume the value of zero at  $t = 0$  and will eventually equate to  $h$ . It is also clear that since  $i \geq s$  the condition  $i = h$  is realized earlier than  $s = h$ .

The process of consolidation has three distinctive phases (mathematically speaking). Phase I defined by  $i \leq h$  takes place during the period from  $t = 0$  to  $t_{i=h}$ . At the end of this phase,  $s$  has a value of  $s_{i=h}$ . Phase II is defined by  $s_{i=h} < s \leq h$  and progresses during this period from  $t_{i=h}$  to  $t_{s=h}$ . Phase III is defined by  $i = s = h$  and the process continues from  $t_{s=h}$  to  $t \rightarrow \infty$ . Each of the above three phases must be treated separately.

#### Phase I

The set of equations governing the process is:

$$\left. \begin{aligned} (\delta/\delta t)\sigma_1 &= \alpha_1(\delta^2/\delta z^2)\sigma_1 \text{ for } 0 < z < s & (a) \\ (\delta/\delta t)\sigma_2 &= \alpha_2(\delta^2/\delta z^2)\sigma_2 \text{ for } s < z < i & (b) \\ \sigma_1(0, t) &= w & (c) \\ \sigma_2(i, t) &= -v & (d) \\ (\delta/\delta z)[\sigma_2(i, t)] &= 0 & (e) \\ (\delta/\delta z)\sigma_1(s, t) &= (\delta/\delta z)\sigma_2(s, t) & (f) \\ \sigma_1(s, t) &= \sigma_2(s, t) = 0 & (g) \end{aligned} \right\} I$$

where  $w = \sigma_f - \sigma_0$  and  $v = \sigma_0 - \sigma_i$  are constant and where use has been made of a new parameter  $\sigma = \sigma' - \sigma_0$ . Subscripts 1 and 2 refer, respectively, to the portion of the layer that has become normally consolidated and to the portion that is still overconsolidated. Parameter  $\alpha$  represents the coefficient of consolidation of the clay.

Integration of (I,a) with respect to  $z$  between limits  $z = 0$  to  $z = s$  yields:

$$(4) \quad \frac{1}{\alpha_1} \frac{d\theta_1}{dt} + \frac{\delta}{\delta z} \sigma_1(0, t) = \frac{\delta}{\delta z} \sigma_1(s, t)$$

where

$$(5) \quad \theta_1 = \int_{0_i}^s \sigma_1 dz$$

also if

$$(6) \quad \theta_2 = \int_s^i \sigma_2 dz.$$

A similar integration of (I,b) between limits of  $z = s$ , to  $z = i$  yields, after some simplification,

$$(7) \quad \frac{\delta}{\delta z} \sigma_2(s, t) = \frac{-1}{\alpha_2} \frac{d}{dt} (\theta_2 + iv).$$

Combining (4) and (7) and using condition (I, f)

$$(8) \quad \frac{1}{\alpha_1} \frac{d\theta_1}{dt} + \frac{1}{\alpha_2} \frac{d}{dt} (\theta_2 + iv) + \frac{\delta}{\delta z} \sigma_1(0, t).$$

Let

$$(9) \quad \sigma_1 = a_1(t) + b_1(t)z + c_1(t)z^2$$

and assume a corresponding expression with coefficients  $a_2$ ,  $b_2$ , and  $c_2$  for  $\sigma_2$ . Substituting these forms of  $\sigma_1$  and  $\sigma_2$  in equations (5), (6), and (7) and using the boundary conditions (I,c), (I,d) and (I,g) result in the set of equations:

$$\left. \begin{aligned} \frac{1}{\alpha_2} \frac{d}{dt} (\theta_2 + iv) + \frac{1}{2\alpha_1} \frac{d\theta_1}{dt} - \frac{w}{s} &= 0 \\ \theta_1 &= \frac{1}{2} \left[ ws - \frac{s^2}{6\alpha_1} \frac{d\theta_1}{dt} \right] \\ \theta_2 &= \frac{-1}{3\alpha_2} \left[ \frac{d}{dt} (\theta_2 + iv) \right] (i - s)^2 \\ (i - s) \frac{d}{dt} (\theta_2 + iv) &= 2v\alpha_2. \end{aligned} \right\} \text{II}$$

The original set of partial differential equations has now been transformed into a set of simultaneous ordinary differential equations that must be solved with the initial conditions  $\theta_1 = \theta_2 = i = s = 0$  at  $t = 0$ . Although the variables in II are non-linearly coupled, a simple solution of the set in fact exists. For variables  $i$  and  $s$  this solution assumes the form

$$(10) \quad i = ms$$

$$(11) \quad s = Mt^{\frac{1}{2}}$$

where  $m = m(\mu, \beta)$  and  $M = M(\mu, \beta)$  are independent of time but are functions of dimensionless parameters  $\mu$  and  $\beta$  defined by  $\mu = (\alpha_1/\alpha_2)$  and  $\beta = (v/w)$ . Parameters  $m$  and  $M$  must satisfy the conditions,

$$(12) \quad 12\alpha_2 = M^2(m - 1)(m + 2)$$

$$(13) \quad [2(m - 1)(m + 2)\mu + 1][(m - 1) - 4\beta] = 6(m - 1).$$

Equation (13) has three roots, two of which are always smaller than unity but the third of which is always larger; it is this root that must be used in (10) since, as mentioned above,  $i \geq s$ .

### Phase II

Proceeding in exactly the same manner as above or alternatively by putting  $i = h$  in the first and third equation of II, a set of simultaneous ordinary differential

equations results, which upon substitution for  $\theta_1$ ,  $\theta_2$  and  $s$  and  $t$  in terms of dimensionless variable  $X, Y, Z$  and  $\tau$ , reads as follows:

$$\left. \begin{aligned} 2\mu \frac{dY}{d\tau} + \frac{dX}{d\tau} - \frac{2\mu}{Z} &= 0 \\ 2X &= \left[ Z - \frac{Z^2}{6\mu} \cdot \frac{dX}{d\tau} \right] \\ Y &= \frac{1}{3} \frac{dY}{d\tau} (1 - Z)^2 \end{aligned} \right\} \text{III}$$

where  $X = (\theta_1/wh)$ ,  $Y = (\theta_2/wh)$ ,  $Z = (s/h)$ , and  $\tau = (\alpha_2/h^2)t$ . The appropriate initial conditions are determined from the values of  $\theta_1$ ,  $\theta_2$  and  $s$  obtained at the termination of Phase I. Unfortunately a simple analytical solution of III has not been found, and a series form or a numerical technique must be adopted. The latter technique has been used in the particular example given in the text.

*Phase III*

This phase of the process starts when  $t_s = h$ . The problem is no longer non-linear because of the absence of the unknown variable  $s$ . The consolidation process is simply governed by equation (I,a) with boundary conditions (I,c) and the condition  $(\delta/\delta Z) \sigma, (h,t) = 0$ . The initial condition is determined from the form of  $\sigma$ , at the time  $t = t_s = h$ , i.e., the end of Phase II of the process. As the problem is linear from this point on, any standard technique (such as the application of the Laplace Transform) may be used to obtain the solutions.

In Figure 12 the distribution of pore water pressure for the case  $\beta = .75$  and  $\mu = \frac{1}{2}$  has been represented. The solid curves correspond to the same sample configuration and mode of loading as when normally consolidated throughout the process. The effect of the overconsolidation is quite clear; up to the end of the second phase, the rate of dissipation of the pore water pressure has been nearly twice as fast as the corresponding rate, had the sample been normally consolidated.

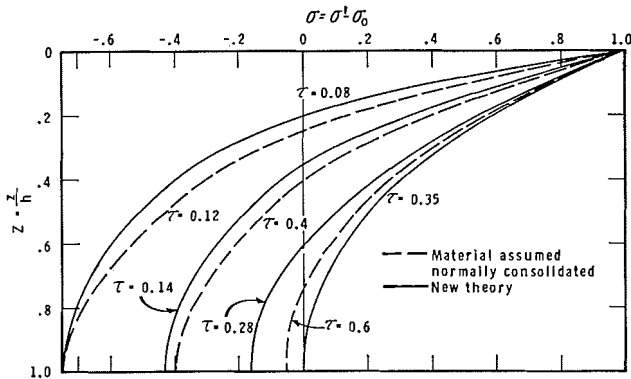


FIGURE 12. Time factors for distribution of pore water pressure

If the clay material is assumed to be rigid plastic (plastic in a broad sense), then equations (I,a) and (I,b) would reduce to

$$(\delta\sigma_1/\delta t) = (\delta u/\delta t) = \infty.$$

In other words, Phases I and II would be completed in an infinitesimal time period. Physically this means that the clay would momentarily experience the high initial imposed pore water pressure but would immediately dissipate it to the level of  $v$ . This assumption has been made in the above case history and the results appear to be in agreement with theory.

The mode of application of the "heat balance integral" technique is potentially extensive and is a powerful tool for solving linear and non-linear consolidation problems. The basic aim of this Appendix has been to demonstrate the application of the "heat balance integral" technique to the solution of a typical consolidation problem. The exact nature of the problem is incidental; in fact, the set of equations I (with appropriate conditions employed in lieu of I,d and I,c) can be rewritten in their finite difference forms and the resulting set of algebraic equations solved by any technique of successive approximations (see, for example, Raymond 1966).

#### REFERENCES

- GOODMAN, T. R., 1964. Contribution to *Advances in Heat Transfer* (Academic Press, New York): 52-120.
- RAYMOND, G. P., 1966. Consolidation of slightly overconsolidated soils. *JSM&FD, Proc. ASCE* 92, SM5.